

**Sensor properties of Pd doped SnO₂ nanofiber enshrouded with
functionalized MWCNT**

Cihat Tasaltin*

TÜBİTAK Marmara Research Center, Materials Institute, P.O Box 21

41470 Gebze, Kocaeli, Turkey

*** Corresponding Author**

Dr. Cihat Tasaltin

Tel: +90 262 677 3042

Fax: +90 262 677 2309

E-mail address: cihat.tasaltin@tubitak.gov.tr

Abstract In this work, tin oxide (SnO₂)/multi-walled carbon nanotube (MWCNT) composite based ethanol sensor that exhibits fast response/recovery behaviour, large sensitivity, and good selectivity was demonstrated. First, Pd doped SnO₂ (SnO₂-Pd) nanofibers was prepared on the interdigitated electrodes (IDE) using electrospinning technique, followed by calcination at 600 °C for 2 h. Then, carboxylic acid modified multi-walled carbon nanotube (MWCNT-COOH) was dropped on the nanofibers and allowed to dry at RT. Next, the thin films were characterized by field emission scanning electron microscopy (FE-SEM), transmission electron microscopy (TEM), X-ray diffraction (XRD) and thermogravimetric analysis (TGA). Finally, chemical sensing behaviors of the sensors were analyzed against to ethanol (ETH), toluene (TOL), trichloroethylene (TCE), acetone (ACE) and binary mixing with water. It was demonstrated that increasing the temperature and gas concentration has led to increased sensor response for SnO₂-Pd nanofiber system. However, there was no general rule found for MWCNT-COOH coated SnO₂-Pd nanofiber system. A novel sensing mechanism was offered for the composite structure.

Keywords: Flexible sensor, VOC sensing, multi-walled carbon nanotube, gold nanoparticle, polyimide

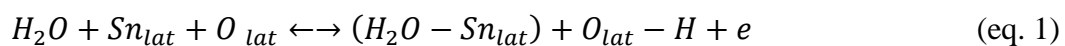
1. Introduction

Oxide semiconductor gas sensors undergo resistance change upon exposure to reducing gases by oxidative interactions with the negatively charged chemisorbed oxygen. The gas sensing characteristics such as gas response, responding speed, and selectivity are greatly influenced by the surface area, donor density, agglomeration, porosity, acid–base property of the sensing material, the presence of catalyst and the sensing temperature[1]. Tin oxide (SnO_2), n-type wide-gap semiconductor, is regarded as an important functional material for gas sensor applications owing to its small size, lightweight and simple fabrication procedures[2]. In addition, SnO_2 are frequently doped with noble metals such as palladium (Pd), platinum (Pt) and gold (Au) to promote the sensing properties such as selectivity, sensitivity and lower working temperature[3]. The form of sensing material is also another parameter for the sensors. For instance, one dimensional (1-D) structures such as nanofiber, nanobelt and nanowire has many advantages during sensing since 1-D structure can provide excellent electron transfer properties due to their large surface area to volume ratio, high porosity and higher gas diffusion area [4]. Among the 1-D materials, nanofibers have attracted great attention due to the simplicity in preparation.

Electrospinning is a widely utilized simple and economical method for producing nanofibers. In the past years, it was mainly used for preparation of pure organic polymer nanofibers[5, 6]. Recently, functional ceramic nanocomposite fibers, such as CuO, SnO_2 , TiO_2 , ZnO, CeO_2 , Ta_2O_5 , Nb_2O_5 and TaNbO_5 were prepared via electrospinning of metal precursor incorporated polymer solution [6-9]. In a typical electrospinning process, nanofibers are produced by applying high voltage to the viscous polymer solution [7]. Under the effect of a strong electric field, a droplet is formed at the end of metal tip. The droplet experiences two major types of electrostatic force: a Columbic force exerted by the external electric field and an electrostatic

repulsion between surface charges [10]. With these electrostatic interactions, the droplet is ejected into a conical object (known as Taylor cone). When the applied voltage reaches a critical value, the electrostatic forces overcome the surface tension of the solution and an electrified jet is produced, which in turn led to formation of continuous nanofibers [7]. Nanofibers, which were produced using electrospinning technique, have been used for various applications such as gas sensor, filtration, biomaterial devices, tissue engineering, and photovoltaics [11-13].

Up to date, doped and undoped SnO₂ in various forms such as nanoparticle, nanofiber and nanohollow have been synthesized and used for detection of ethanol, H₂ and NH₃ by various research groups. In addition, Pd doped SnO₂ has been used for CO sensors by Gaidi *et al*[14]. Regardless of doping, SnO₂ is known to be very sensitive to moisture. Interaction of SnO₂ with the humidity was explained in detail in previous works by Heiland and Barsan [15-18]. According to the reports, there are two main significant mechanisms that play key role between the humidity and SnO₂. Firstly, water molecule can be adsorbed by the SnO₂ surface either as a molecule or as a hydroxyl group. If adsorption happens below 400 °C, no effect on conductivity is observed. If adsorption occurs via chemisorption of hydroxyl groups, the resistance is reduced and this species is not completely desorbed even at 600 °C. Heiland suggests two interaction mechanisms of water molecule; 1) dissociation or 2) reduction. In the former one, water molecules adsorbed by the surface results in hydrogen bonding and electron release. In the latter one, water molecule with two hydroxyl groups, rooted one including lattice oxygen another one bound to lattice tin. These phenomena can be expressed by the following equations[15].



On the other hand, small molecules such as methane, acetic acid and ethanol have an interaction with SnO₂ based on decomposition and oxidation processes [15]. Therefore, to obtain distinct sensor responses against to VOCs, SnO₂ has been doped by various metals.

Conductivity of these materials has been discussed in the context of an activated tunneling model as defined in Eq. 3.

$$\sigma \approx \exp(-\beta\delta) \exp\left(\frac{-E_a}{KT}\right) \quad (\text{eq. 3})$$

where β , δ , E_a and k_b represents the tunneling decay constant, edge-to-edge separation of the metal cores, activation energy, Boltzmann constant, respectively. The first term defines the tunneling current between the neighboring of sensing material, which decreases with increasing particle distance [19]. The second term describes the thermal activation of charge carriers in which Arrhenius term is inversely proportional to the permittivity of the organic matrix. According to the equation, conductivity is also dependent of the dielectric constant of the analyte which was ascribed to a change in permittivity of the matrix as the dominating component of sensing mechanism [20, 21].

In this work, it was attempted to prepare Pd doped SnO₂ (SnO₂-Pd) nanofiber enshrouded with MWCNT-COOH layers to block the interference of humidity and other gases on sensor responses. To fabricate SnO₂-Pd nanofiber, electrospinning method was utilized. It is well known that, resistivity of MWCNT-COOH layer increases with the humidity because the adsorbed water molecules inside the MWCNT-COOH layer makes it difficult for the electrons to transport between the nanotubes [22, 23]. Other advantage of the MWCNT-COOH layer could be the effect of defects on the nanotubes in the sensing of polar molecules such as water and ethanol. Watt reported oxygen containing defects withdraws electron density from the nanotubes which increases the number of hole carriers and makes the nanotubes p-type with lower resistivity. Upon the adsorption of water molecules on the oxygen containing defects,

electron-withdrawing power of the electronegative functional groups (i.e. carboxyl and epoxide) reduces, which in turn led to increased resistance [24].

2. Materials and methods

2.1 Materials and sensor fabrication

200 mg $\text{SnCl}_2 \cdot 2\text{H}_2\text{O}$ (98 %, Sigma-Aldrich) was dissolved in 5 ml methanol and stirred for 1 h, followed by adding 200 mg Polyvinylpyrrolidone (PVP, Mw: 1.300.000 g/mol, Sigma-Aldrich) to the solution and stirring for 1 h (weight ratio 1:1). For the preparation of Pd doped SnO_2 nanofiber, 8 mg PdCl_2 (99,99 %, Sigma-Aldrich) was added to the above solution and stirred for 1 h. Subsequently, the resulting solution was loaded into a plastic syringe and electrified using a high-voltage DC supply. As demonstrated in Fig. 1, the electrospinning equipment is a two-compartment setup with a sample holder that rotates at a velocity of 1.000 rpm, exposing the IDE to the positive electrospay mist and a negative discharge cloud. The coating voltages were adjusted to $\sim +3,5$ kV for the needle and $\sim -1,5$ kV for the tungsten tip [25, 26]. After the electrospinning process, the nanofibers were subjected to calcination at 600 °C in air for 2 h to remove the PVP and crystallize the SnO_2 . To measure the sensor properties, an interdigitated electrode (IDEs) which consists of titanium finger pairs on Si/ SiO_2 substrate with the following dimensions; 10 μm electrode width, 10 μm spacing and 2 μm electrode thickness were used.

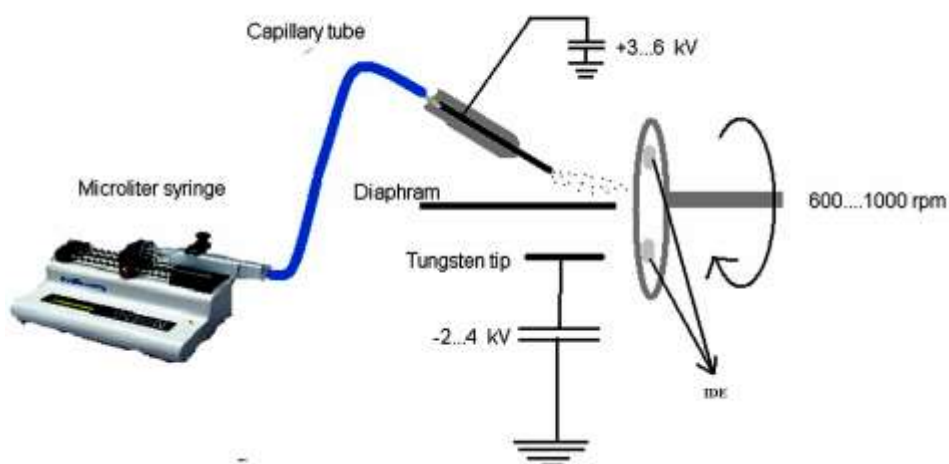


Figure 1. The electrospinning system[26]

Finally, carboxylic acid modified multi-walled carbon nanotubes (MWCNT-COOH, Nanoshel, US) solution was prepared in methanol. 10-15 μl portions was simply dropped on SnO_2 layer and allowed to dry at RT.

2.2 Characterization

Synthesized SnO_2 -Pd nanofibers were characterized by X-ray diffractometer (XRD, Shimadzu XRD-6000), transmission electron microscopy (TEM, JEOL 2100) and thermogravimetric analysis (TGA, Seiko Exstar 6300) while the morphology of the sensing layers was analyzed by field emission scanning electron microscopy (FE-SEM, JEOL 63335F)

2.3 Sensor measurement

Chemical sensing behaviors were analyzed against polar (water, propanol and ethanol) and nonpolar (hexane, toluene, trichloroethylene and chloroform) volatile organic compounds (VOCs). The gas stream containing VOC vapor was generated from cooled bubblers that were

immersed in a thermally controlled bath with synthetic air as the carrier gas. The gas stream saturated with the analyte was diluted with pure synthetic air to adjust the gas concentration to the desired amount by using computer driven mass flow controllers (MKS Instruments Inc., USA) at a constant flow rate of 200 ml/min. Typical experiments consisted of repeated exposure to the analyte gas (10 min) and a subsequent purging with pure air (10 min) to reset the baseline. The measurements were performed under individual and binary mixtures of VOC and humidity while the component of gas concentrations were varied in the range of 100–5000 ppm (Table 1). The binary measurements were taken under constant humidity and changing VOC concentrations. Meanwhile, the humidity levels were kept at 0, 30, 50 and 75 % relative humidity (RH) for each binary measurements. The temperature of the sensor chip was kept at 200, 250 and 300 °C with the help of temperature controller (Lake Shore, USA). Electrical resistances (DC) were measured with a programmable electrometer (Keithley 617). Instruments were controlled and read by computer using a GPIB interface.

For a better comparison, the responses of different vapor pressures' relative concentrations p_i/p_{0i} are used, where p_i is the actual analyte concentration and p_{0i} is the saturation vapor pressure at the measurement temperature [25].

Table 1. Properties of analytes, the tested concentration range, saturation vapor pressure at $-10\text{ }^{\circ}\text{C}$

Analyte	Dielectric constant (ϵ)	Dipole Moment (μ)	Concentration (ppm)		$p^0(-10\text{ }^{\circ}\text{C})$ ppm
			Min.	Max.	
Toluene (TOL)	2.38	0.26	120	1200	4920
Trichloroethylene(TCE)	3.40	0.81	550	3100	15800
Acetone (ACE)	6.2	2.91	1440	1152	28800
Ethanol (ETH)	24.50	1.69	460	2300	9200
Water	80.10	1.85			

The response of sensors to the various gas environments is defined as $S = \frac{\Delta R}{R_0} = \frac{R_g - R_0}{R_0}$ where R_g is the resistance when exposed to gas environments, R_0 is the resistance of the baseline in the dry air or continued humid air. The S value is represented as sensitivity in the literature; however, this should be defined as the deviation from the baseline.

Sensitivity of sensor can be defined as follows [27];

$$\bar{S} = \frac{1}{nR_0} \sum_{i=1}^n \frac{(R_{gi} - R_{g(i-1)})}{(C_{gi} - C_{g(i-1)})} \quad (\text{eq. 4})$$

where C_{gi} represents the concentration for the applied gas, R_{gi} is the measured resistance for the applied gas concentration and n is the number of applied concentrations. If $i=1$ then $R_{g0} = R_0$ and $C_{g0} = 0$. This approach gives the concentration of the detected gas per one unit changes.

3. Results and Discussion

3.1 Morphological and physical characterizations

It is well known that the sensing layer plays a crucial role in the sensors and its structural and chemical characteristics will directly affect the sensing performance. TEM analysis (Fig. 2-a) reveal that the nanofibers involve a granular crystalline microstructure with tiny nanograins. In addition, nanofibers include only tin, oxygen and palladium atoms, which demonstrates the absence of the impurities (Fig. 2-b), indicating the successful removal of organics with calcination.

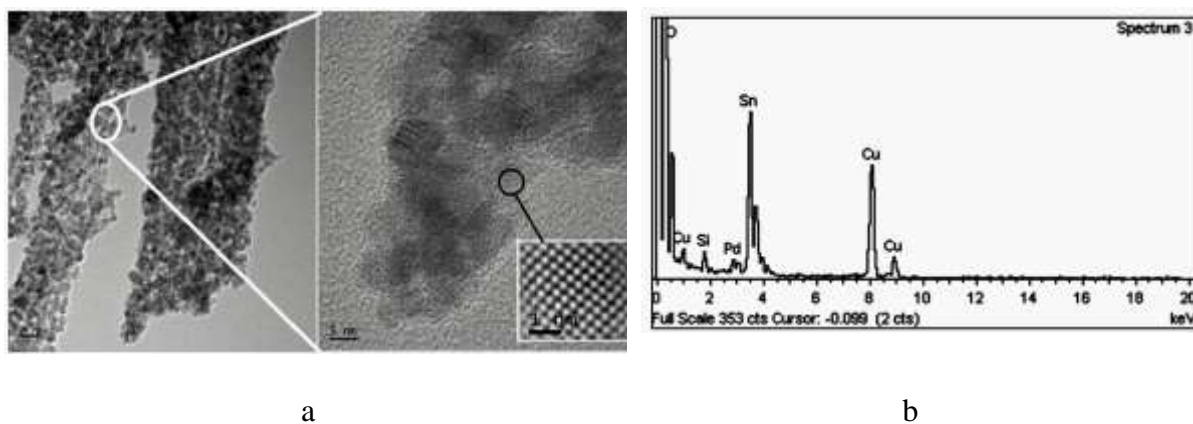


Figure 2. a) TEM image and b) EDS spectrum of SnO₂-Pd nanofiber

As revealed by SEM analysis (Fig. 3-a), SnO₂-Pd nanofiber layer exhibits continuous interconnected network structure with a fiber diameter of 50-100 nm, which proves the successful electrospinning process. In addition, it was demonstrated that MWCNT-COOH layer were homogeneously coated on the nanofiber layer (Fig. 3-b).

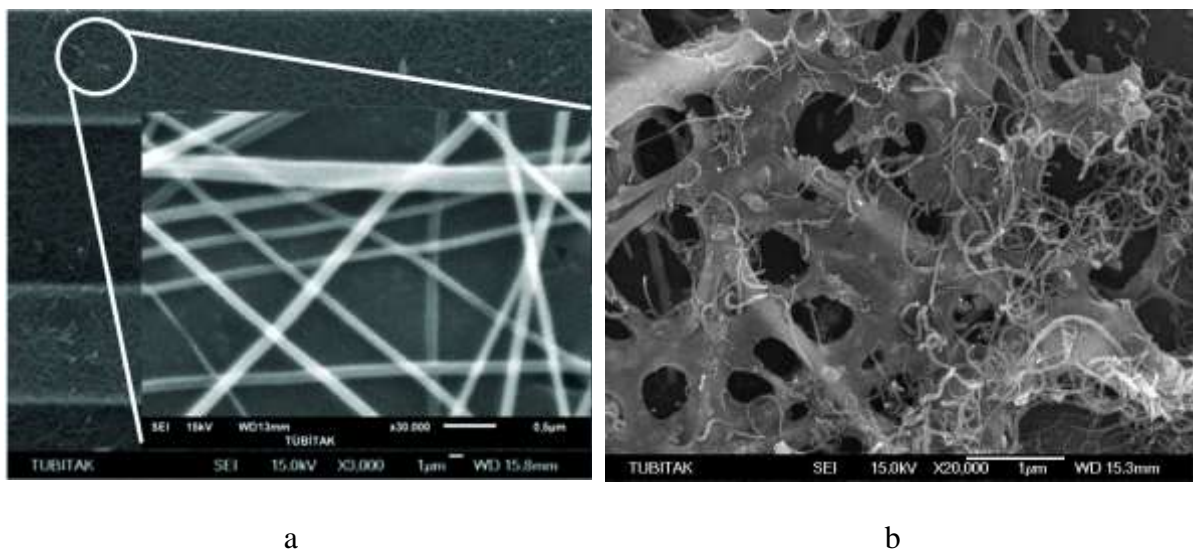


Figure 3. SEM image of a) SnO₂-Pd nanofiber layer b) MWCNT-COOH layer on nanofibers

On the other hand, crystalline structure of the SnO₂-Pd nanofibers was investigated by XRD. It is obvious that nanofibers show polycrystalline structure (Fig. 4-a), demonstrating the successful calcination process (600 °C) in agreement with previous works[12, 28]. The formation of polycrystalline structure could be attributed to the removal of PVP and oxidation of tin element. No peaks from either any other phase of SnO₂ or any impurities were observed. Moreover, TGA analysis was carried out to investigate the thermal degradation behavior of PVP during calcination process. As shown in Fig. 4-b, the weight loss increases dramatically with increasing the temperature and levels off at 400 °C, which can be explained by the removal of all organics. This again indicates the successful calcination process and formation of pure SnO₂ nanofibers[29].

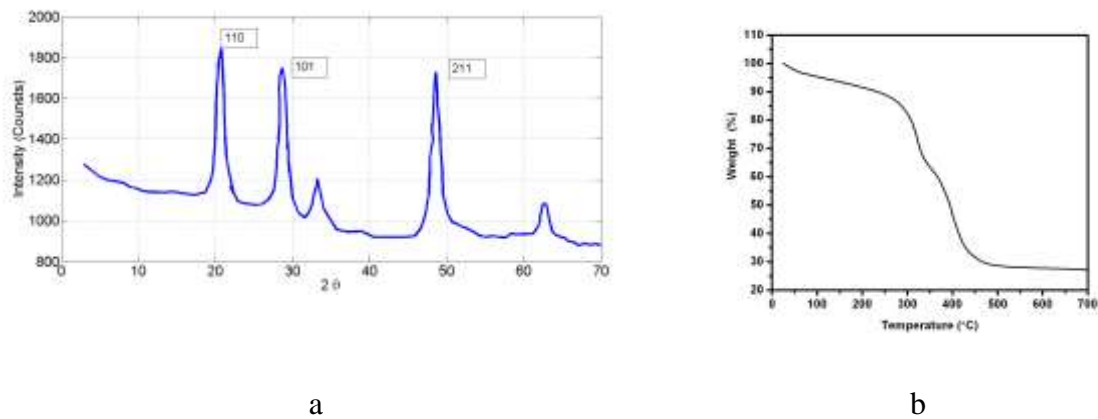


Figure 4. a) XRD spectrum SnO₂-Pd nanofiber after calcination and b) TGA analysis of SnO₂-Pd nanofiber before calcination at 600 °C.

3.2 Characterization of sensor responses

3.2.1 Ethanol sensing

Ethanol responses of the SnO₂-Pd sensors as a function of temperature were shown in Figure 5a. The sensor response is almost negligible at 200 °C, however, increasing the temperature resulted in better sensor response. On the other hand, the sensor response increased dramatically after coating with MWCNT-COOH layer. This could be explained by the support of carbon nanotubes to the electron transfer from SnO₂-Pd nanofibers to the IDE electrodes during sensing (Figure 5b). It can be deduced that all fibers were involved in sensing even if there is no connection between each other or the IDE electrodes.

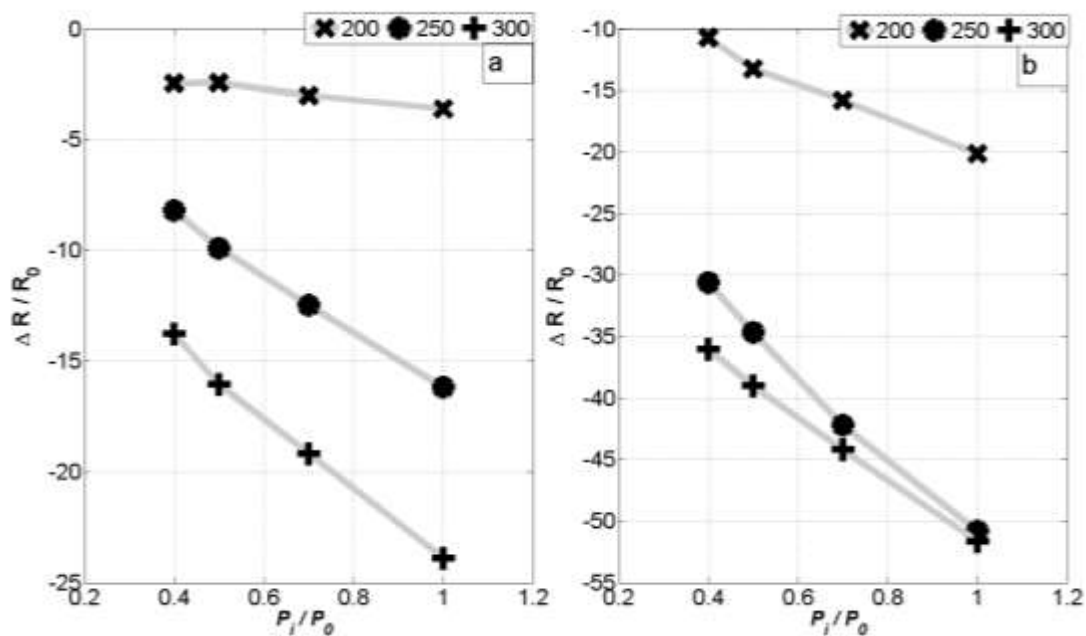
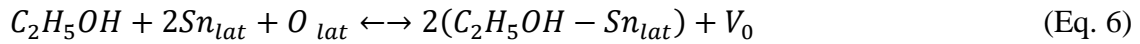


Figure 5. Sensor responses of a) SnO₂-Pd nanofibers and b) MWCNT-COOH coated SnO₂-Pd nanofiber sensors

The sensing mechanism of SnO₂-Pd nanofiber system is based on the interaction between the lattice and -OH groups of ethanol. We believe that the detection of ethanol is similar to water. Size of ethanol molecule is larger than the water molecule; therefore, interaction of ethanol occurs on the surface of SnO₂-Pd nanofiber and generates the electron according to Eq. 1 and 2.



or



Sensing mechanism of the MWCNT-COOH coated SnO₂-Pd nanofiber sensor could be explained by the previous work by Sin *et al*[30]. Owing to its hydroxyl group, ethanol might interact with carboxylic group of carbon nanotubes via hydrogen bonding[24]. This may lead to diminish the number of free charge carriers-holes and thus increase the electrical resistance upon ethanol exposure[30]. It is obvious that the mechanisms mentioned above works opposite to each other. Upon the adsorption of ethanol on the nanofibers, oxide structure generates electrons and injects into the MWCNT-COOH layer. It seems that the number of electrons generated by the nanofibers is higher than the holes that was generated via interaction of ethanol with carbon nanotubes. Hence, an increase in the electrical conductivity was observed for all tests.

Influence of temperature on the electrical conductivity and sensing behavior is another issue that should be considered. Based on the previous works [16, 31], the conductivity of both SnO₂-Pd and MWCNT-COOH layers and thus, sensor baseline is expected to increase by increasing the temperature. Nevertheless, sensor responses of the layers are different due to the dissimilar sensing mechanism, as shown in Figure 6.

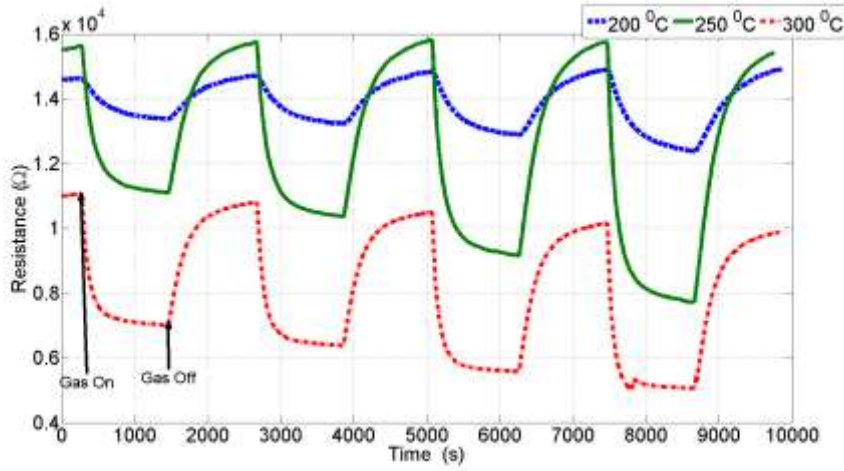


Figure 6. Ethanol response of MWCNT-COOH coated SnO₂-Pd sensor at 200, 250 and 300 °C.

The change in the conductivity and in the sensing behavior of the composite structure with temperature could be understood with the following explanations. There are two different effects in the sensing mechanism. First one is the positive effect on the electrical conductivity upon the interaction of the ethanol with SnO₂ (See Eq. 5 and 6). Second one is the negative effect of the carboxylic group of MWCNT-COOH due to its electronegativity. The carboxylic groups attract the free electrons that interact with SnO₂ structure, which in turn led to decrease in conductivity. Therefore, the sensing mechanism of SnO₂ nanofiber and composite structure (MWCNT-COOH coated SnO₂) is expected to be different.

If there were only SnO₂ nanofibers in the system, the conductivity would increase with temperature (Eq. 3) and interaction with the gas (Eq. 5 and 6). However, adding MWCNT-COOH to the system means adding binary structure which both increases and decreases electrical conductivity.

Sum of both cases define the system's total behavior. Hence,

$$\sigma_{CNT-COOH} = \sigma_{T(CNT-COOH)} - \sigma_{S(CNT-COOH)} \quad (\text{Eq. 7})$$

where $\sigma_{T(CNT-COOH)}$ and $\sigma_{S(CNT-COOH)}$ defines the conductivity change with temperature and interaction with the gases. Minus term demonstrates that the MWCNT-COOH absorbs some of the electrons released after interaction with the gas.

$$\sigma_{SnO_2} = \sigma_{T(SnO_2)} + \sigma_{S(SnO_2)} \quad (\text{Eq. 8})$$

However, Eq. 8 shows that the conductivity increases both with temperature and interaction with the gas. Therefore, the total behavior of the MWCNT-COOH coated SnO₂ nanofiber system could be explained as follows;

$$\sigma_{TOTAL} = \sigma_{T(CNT-COOH)} + \sigma_{T(SnO_2)} + \sigma_{S(SnO_2)} - \sigma_{S(CNT-COOH)} \quad (\text{Eq. 9})$$

where σ_{TOTAL} is the total conductivity of during gas exposure.

3.2.2 Ethanol sensing with humidity

Effect of humidity on the ethanol sensing was also investigated. There is a slight decrease (~1-3 %) in the sensor response when humidity was incorporated in the ethanol, as shown in Figure 7. Since the interaction mechanism of humidity and ethanol with SnO₂-Pd structure is similar, most of the interaction sites were occupied by the water molecules, which led to a decrease in ethanol response. As the temperature was increased, it was found that the sensitivity as also increased, which could be explained by the increased number of sensing sites [32].

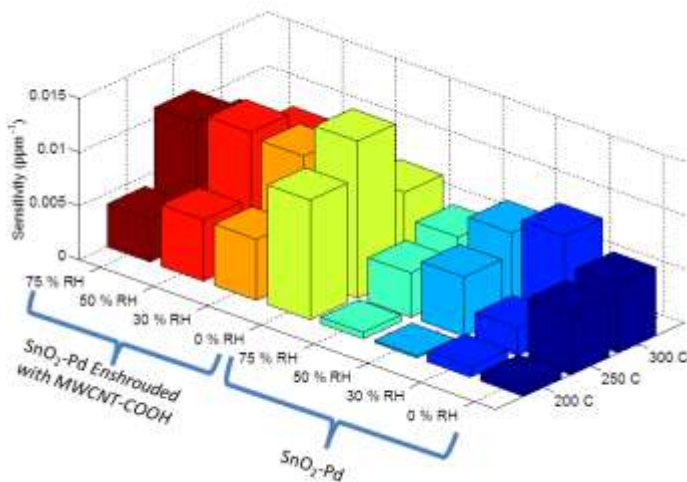


Figure 7. Sensitivity values of SnO₂-Pd nanofiber layer and MWCNT-COOH coated nanofiber layer against ethanol with different humidity levels (calculated with eq. 4)

The sensing mechanism of the enshrouded SnO₂-Pd structures can be explained by eq. 9. Based on this equation, it can be deduced that the generated electrons with temperature increase was absorbed by the MWCNT-COOH layer. In this study, maximum sensitivity against ethanol was achieved at 250 °C for all humidity levels.

nanofiber layer against ethanol with different humidity levels (calculated with eq. 4)

3.2.3 Sensing behaviour of other gases

As demonstrated in Figure 8a, when the SnO₂-Pd nanofiber sensor was exposed to acetone at 200 °C, no response was detected. Increasing the temperature has very small influence on the sensor response. This could be attributed to the absence of proper functional group of acetone that could interact with SnO₂-Pd surface. The behavior of TOL and TCE was also found to be similar (not shown here).

On the other hand, there are increased responses for MWCNT-COOH coated SnO₂-Pd nanofiber layer (Figure 8b and Figure 9b). Carbon nanotubes helps the electron transfer generated during sensing process and sensitivity values increase order of $\sim 10^3$ (Compared to Fig. 8-a and 9-a). Considering these issues, it can be concluded that MWCNT layer works as a filter for the underlying SnO₂ nanofiber layer as well as it works as a sensing layer.

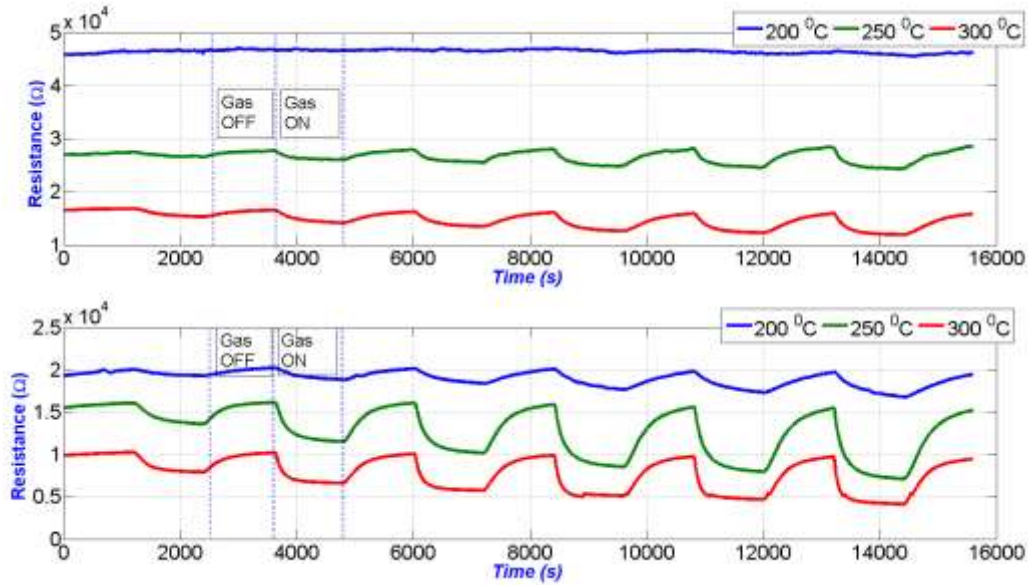


Figure 8. Acetone responses for two sensor structures at different temperature a) SnO₂-Pd nanofiber and b) Enshrouded SnO₂-Pd nanofiber with MWCNT-COOH.

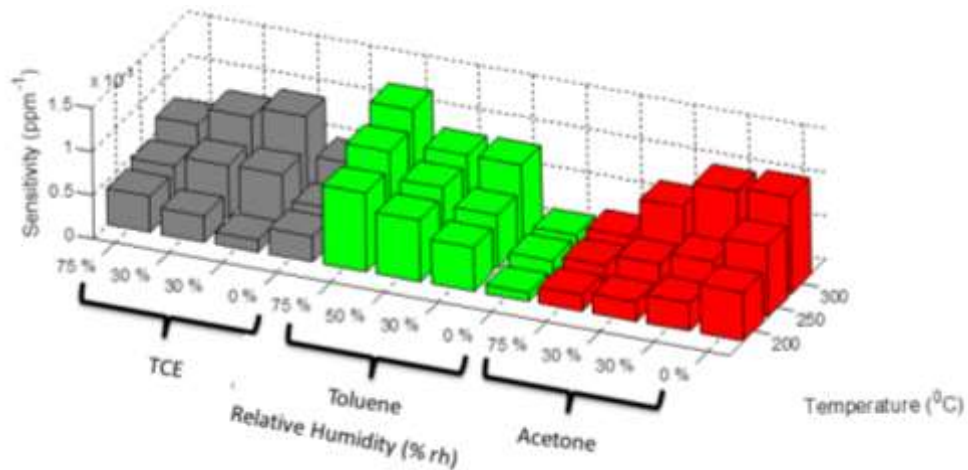


Figure 9. Sensitivities of the sensors at different temperature and humidity levels a) SnO₂-Pd nanofiber b) Enshrouded SnO₂-Pd nanofiber with MWCNT-COOH.

Conclusions

In this work, preparation of ethanol sensor based on SnO₂-Pd/MWCNT-COOH composite structure was successfully achieved. Increasing the temperature and gas concentration has led to increased sensor response for SnO₂-Pd nanofiber system. However, there is no general rule for MWCNT-COOH coated SnO₂-Pd nanofiber system. Sensing mechanisms was modeled for

electrical charge transfer between nanofibers and nanotubes. We have systematically investigated the effect of sensing layer composition on the sensing mechanism.

Acknowledgement

The author would like to acknowledge the financial support from TÜBİTAK (Grant No:115E045).

References

[1] J.-K. Choi, I.-S. Hwang, S.-J. Kim, J.-S. Park, S.-S. Park, U. Jeong, Y.C. Kang, J.-H. Lee, Design of selective gas sensors using electrospun Pd-doped SnO₂ hollow nanofibers, *Sensors and Actuators B: Chemical*, 150 (2010) 191-199.

[2] R.-q. Tan, Y.-q. Guo, J.-h. Zhao, Y. Li, T.-f. Xu, W.-j. Song, Synthesis, characterization and gas-sensing properties of Pd-doped SnO₂ nano particles, *Transactions of Nonferrous Metals Society of China*, 21 (2011) 1568-1573.

[3] W. Li, C. Shen, G. Wu, Y. Ma, Z. Gao, X. Xia, G. Du, New Model for a Pd-Doped SnO₂-Based CO Gas Sensor and Catalyst Studied by Online in-Situ X-ray Photoelectron Spectroscopy, *The Journal of Physical Chemistry C*, 115 (2011) 21258-21263.

[4] K. Mondal, M.A. Ali, V.V. Agrawal, B.D. Malhotra, A. Sharma, Highly Sensitive Biofunctionalized Mesoporous Electrospun TiO₂ Nanofiber Based Interface for Biosensing, *ACS Applied Materials & Interfaces*, 6 (2014) 2516-2527.

[5] X. Yang, C. Shao, Y. Liu, R. Mu, H. Guan, Nanofibers of CeO₂ via an electrospinning technique, *Thin Solid Films*, 478 (2005) 228-231.

[6] N. Dharmaraj, C. Kim, K. Kim, H. Kim, E. Suh, Spectral studies of SnO₂ nanofibres prepared by electrospinning method, *Spectrochimica Acta Part A: Molecular and Biomolecular Spectroscopy*, 64 (2006) 136-140.

[7] Y. Zhang, J. Li, G. An, X. He, Highly porous SnO₂ fibers by electrospinning and oxygen plasma etching and its ethanol-sensing properties, *Sensors and Actuators B: Chemical*, 144 (2010) 43-48.

- [8] X. Yang, C. Shao, H. Guan, X. Li, J. Gong, Preparation and characterization of ZnO nanofibers by using electrospun PVA/zinc acetate composite fiber as precursor, *Inorganic Chemistry Communications*, 7 (2004) 176-178.
- [9] O. Katsuhiko, D. Bin, T. Yosuke, N. Takayuki, Y. Michiyo, S. Shinichiro, O. Shingo, Y. Masato, S. Seimei, Electrospinning processed nanofibrous TiO₂ membranes for photovoltaic applications, *Nanotechnology*, 17 (2006) 1026.
- [10] D. Li, Y. Xia, Electrospinning of Nanofibers: Reinventing the Wheel?, *Advanced Materials*, 16 (2004) 1151-1170.
- [11] Z. Liu, D.D. Sun, P. Guo, J.O. Leckie, An efficient bicomponent TiO₂/SnO₂ nanofiber photocatalyst fabricated by electrospinning with a side-by-side dual spinneret method, *Nano letters*, 7 (2007) 1081-1085.
- [12] J. Huang, N. Matsunaga, K. Shimano, N. Yamazoe, T. Kunitake, Nanotubular SnO₂ templated by cellulose fibers: synthesis and gas sensing, *Chemistry of materials*, 17 (2005) 3513-3518.
- [13] F. Yang, R. Murugan, S. Wang, S. Ramakrishna, Electrospinning of nano/micro scale poly (L-lactic acid) aligned fibers and their potential in neural tissue engineering, *Biomaterials*, 26 (2005) 2603-2610.
- [14] M. Gaidi, B. Chenevier, M. Labeau, Electrical properties evolution under reducing gaseous mixtures (H₂, H₂S, CO) of SnO₂ thin films doped with Pd/Pt aggregates and used as polluting gas sensors, *Sensors and Actuators B: Chemical*, 62 (2000) 43-48.
- [15] G. Heiland, D. Kohl, *Chemical Sensor Technology*, ed., Kodansha, Tokyo, ELSEVIER1988.
- [16] N. Bârsan, U. Weimar, Understanding the fundamental principles of metal oxide based gas sensors; the example of CO sensing with SnO₂ sensors in the presence of humidity, *Journal of Physics: Condensed Matter*, 15 (2003) R813.
- [17] N. Barsan, U. Weimar, Conduction model of metal oxide gas sensors, *Journal of Electroceramics*, 7 (2001) 143-167.
- [18] N. Bârsan, R. Ionescu, The mechanism of the interaction between CO and an SnO₂ surface: the role of water vapour, *Sensors and Actuators B: Chemical*, 12 (1993) 71-75.

[19] Y. Joseph, B. Guse, T. Vossmeier, A. Yasuda, Gold Nanoparticle/Organic Networks as Chemiresistor Coatings: The Effect of Film Morphology on Vapor Sensitivity, *The Journal of Physical Chemistry C*, 112 (2008) 12507-12514.

[20] Y. Joseph, A. Peić, X. Chen, J. Michl, T. Vossmeier, A. Yasuda, Vapor Sensitivity of Networked Gold Nanoparticle Chemiresistors: Importance of Flexibility and Resistivity of the Interlinkage, *The Journal of Physical Chemistry C*, 111 (2007) 12855-12859.

[21] H.L. Zhang, S.D. Evans, J.R. Henderson, R.E. Miles, T.H. Shen, Vapour sensing using surface functionalized gold nanoparticles, *Nanotechnology*, 13 (2002) 439-444.

[22] M. Haichuan, W. Keke, Z. Shicheng, S. Keyi, S. Shaochi, L. Zhi, Z. Jia, X. Haifen, Fabrication and Characterization of Amino Group Functionalized Multiwall Carbon Nanotubes (MWCNT) Formaldehyde Gas Sensors, *Sensors Journal, IEEE*, 14 (2014) 2362-2368.

[23] L. Liu, X. Ye, K. Wu, R. Han, Z. Zhou, T. Cui, Humidity Sensitivity of Multi-Walled Carbon Nanotube Networks Deposited by Dielectrophoresis, *Sensors*, 9 (2009) 1714-1721.

[24] P.C.P. Watts, N. Mureau, Z. Tang, Y. Miyajima, J.D. Carey, S.R.P. Silva, The importance of oxygen-containing defects on carbon nanotubes for the detection of polar and non-polar vapours through hydrogen bond formation, *Nanotechnology*, 18 (2007) 175701.

[25] C. Tasaltin, M.A. Ebeoglu, Z.Z. Ozturk, Acoustoelectric Effect on the Responses of SAW Sensors Coated with Electrospun ZnO Nanostructured Thin Film, *Sensors*, 12 (2012) 12006-12015.

[26] C. Tasaltin, F. Basarir, Preparation of flexible VOC sensor based on carbon nanotubes and gold nanoparticles, *Sensors and Actuators B: Chemical*, 194 (2014) 173-179.

[27] M.E. Franke, T.J. Koplín, U. Simon, Metal and metal oxide nanoparticles in chemiresistors: does the nanoscale matter?, *Small*, 2 (2006) 36-50.

[28] X. Song, Z. Wang, Y. Liu, C. Wang, L. Li, A highly sensitive ethanol sensor based on mesoporous ZnO–SnO₂ nanofibers, *Nanotechnology*, 20 (2009) 075501.

[29] M. Shabanián, N.-J. Kang, D.-Y. Wang, U. Wagenknecht, G. Heinrich, Synthesis, characterization and properties of novel aliphatic–aromatic polyamide/functional carbon nanotube nanocomposites via in situ polymerization, *RSC Advances*, 3 (2013) 20738-20745.

[30] M.L. Sin, G. Chun Tak Chow, G.M. Wong, W. Li, P. Leong, K.W. Wong, Ultralow-power alcohol vapor sensors using chemically functionalized multiwalled carbon nanotubes, *Nanotechnology, IEEE Transactions on*, 6 (2007) 571-577.

[31] Y. Zhang, X. He, J. Li, Z. Miao, F. Huang, Fabrication and ethanol-sensing properties of micro gas sensor based on electrospun SnO₂ nanofibers, *Sensors and Actuators B: Chemical*, 132 (2008) 67-73.

[32] J.F. Boyle, K.A. Jones, The effects of CO, water vapor and surface temperature on the conductivity of a SnO₂ gas sensor, *Journal of Electronic Materials*, 6 (1977) 717-733.